Effect of random background inhomogeneity on observer detection performance

J. P. Rolland*

Optical Sciences Center, University of Arizona, Tucson, Arizona 85721

H. H. Barrett

Optical Sciences Center, University of Arizona, Tucson, Arizona 85721, and Department of Radiology, University of Arizona, Tucson, Arizona 85724

Received May 15, 1991; revised manuscript received October 28, 1991; accepted October 30, 1991

Many psychophysical studies of the ability of the human observer to detect a signal superimposed upon a uniform background, where both the signal and the background are known exactly, have been reported in the literature. In such cases, the ideal or the Bayesian observer is often used as a mathematical model of human performance since it can be readily calculated and is a good predictor of human performance for the task at hand. If, however, the background is spatially inhomogeneous (lumpy), the ideal observer becomes nonlinear, and its performance becomes difficult to evaluate. Since inhomogeneous backgrounds are commonly encountered in many practical applications, we have investigated the effects of background inhomogeneities on human performance. The task was detection of a two-dimensional Gaussian signal superimposed upon an inhomogeneous background and imaged through a pinhole imaging system. Poisson noise corresponding to a certain exposure time and aperture size was added to the detected image. A six-point rating scale technique was used to measure human performance as a function of the strength of the nonuniformities (lumpiness) in the background, the amount of blur of the imaging system, and the amount of Poisson noise in the image. The results of this study were compared with earlier theoretical predictions by Myers *et al.* [J. Opt. Soc. Am. A **7**, 1279 (1990)] for two observer models: the optimum linear discriminant, also known as the Hotelling observer, and a nonprewhitening matched filter. Although the efficiency of the human observer relative to the Hotelling observer was only approximately 10%, the variation in human performance with respect to varying aperture size and exposure time was well predicted by the Hotelling model. The nonprewhitening model, on the other hand, fails to predict human performance in lumpy backgrounds in this study. In particular, this model predicts that performance will saturate with increasing exposure time and drop precipitously with increasing lumpiness; neither effect is observed with human observers.

INTRODUCTION

When assessing image quality in medical imaging, it is useful to compare the performance of mathematical observer models with human performance to determine whether the mathematical observers could be used as a basis for system assessment and optimization.[1,2] Throughout the literature, the most commonly used mathematical observer is the Bayesian or the ideal observer. This choice necessitates the use of stylized tasks, such as the detection of a disk superimposed upon a uniform background and embedded in white Gaussian noise, for which the ideal-observer performance can be readily calculated. The results of many studies carried out for such simple tasks are consistent with the point of view that the human-observer performance correlates well with that of a Bayesian observer,[3-10] but relatively few studies of more complex tasks have been performed. Revesz *et al.*[11] used chest radiographs to measure lesion detection in inhomogeneous, spatially complicated backgrounds. Their model of lesion conspicuity leads to good agreement between conspicuity measurements and human performance, but more rigorous mathematical observers were not considered. The effect of variable-brightness background levels and areas on the detectability of disk signals was studied by Swensson and Judy[12] for the cases of uncorrelated noise and computed tomography noise. Their results did not seem to depend either on the type of image noise or on the value of the mean background brightness. Visual conspicuity and background effects were also studied, for example, by Engel,[13] Cole and Jenkins,[14] Ruttimann and Webber,[15] and Tsui *et al.*[16]

The primary purpose of this study is to determine the performance of human observers on a task in which background complexity is a significant factor but for which mathematical observer models remain tractable. Our approach toward simulating more complex images is to superimpose a given signal upon a nonuniform or a lumpy background, which can be described as a stationary random process. We might consider as possible mathematical observers for this task the ideal Bayesian observer; the nonprewhitening (NPW) matched-filter observer, referred to as the NPW observer; and the Hotelling observer.[17-22] Determination of the performance of the ideal observer requires full knowledge of the probability densities of the images under the two hypotheses. In the case of a lumpy background, we are usually unable to compute the ideal-observer performance since full knowledge of the probability density of the data is generally difficult to derive or even to estimate as the complexity of the task increases.

0740-3232/92/050649-10$05.00

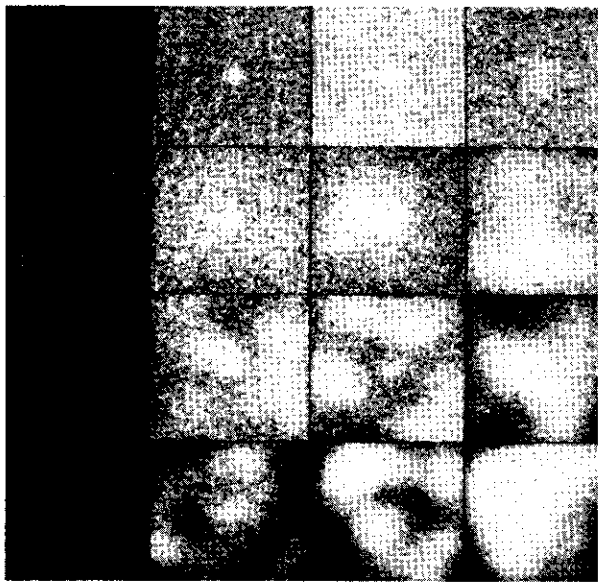

Fig. 1. Illustrative images of a signal on various backgrounds. The leftmost column shows Gaussian pinhole ($r_p = 0.4\ r_s$) images of a Gaussian signal (50% contrast, $r_s = 5.66$ pixels, centered in the object array) superimposed upon lumpy backgrounds with a correlation length of 16.98 pixels for $W_f(0) = 0$, 1.3×10^5, 8.2×10^5, and 3.3×10^6 counts^2/(s^2 pixel) from top to bottom. The second column shows the same objects imaged by a Gaussian aperture with $r_p = 0.8\ r_s$. The third and the fourth columns show the same objects imaged by an aperture size r_p equal to $1.6\ r_s$ and $3.2\ r_s$, respectively. In all the cases the exposure time was set to 1 s.

Therefore we consider the less-demanding Hotelling and NPW observers, for which we need only the first- and the second-order statistics of the data.

Another motivation for investigating the assessment of image quality for more complex images arises from an apparent contradiction between the ideal-observer model and clinical experience in nuclear medicine. In this field, a gamma-ray image of a radioactive organ is formed with a pinhole or similar aperture, and an important practical question is how large to make the aperture. A larger aperture gives better photon-collection efficiency but poorer spatial resolution. If the task is the detection of a completely specified signal in an infinite, uniform background of known strength, the ideal-observer strategy leads to an optimum aperture that is infinite in spatial extent for a given imaging time. In other words, for the task at hand, resolution seems to be useless from an ideal-observer point of view. Similarly, given a finite aperture size, the performance of the ideal observer increases linearly with increasing imaging time,[23,24] so that any desired level of detection performance can be obtained by just increasing the exposure time. The interesting question that then emerges is whether human performance also increases indefinitely with increasing exposure time or aperture size.

We focus in this paper on the two-hypothesis detection task, in which the signal to be detected has a Gaussian profile of constant width and amplitude and is superimposed upon a statistically stationary lumpy background of constant correlation length but of varying lumpiness, where lumpiness can be thought of as the amount and the strength of the background nonuniformities. Typical images are shown in Figs. 1 and 2. The effect of the aperture size on the detection of a signal of known size and contrast that is superimposed upon lumpy backgrounds of a given correlation length but of varying lumpiness is illustrated in Fig. 1, while the effect of the exposure time on detection is illustrated in Fig. 2 for an aperture size that matches the size of the signal.

The theoretical basis for this lumpy-background problem was presented by Myers *et al.*,[25] and the predictions of performance were derived for the Hotelling and the NPW observers. In this paper we seek to determine whether either of these two observer models predicts the performance of human observers. We present two psychophysical studies. In the first study we investigate the importance of aperture size on human-observer performance, and in the second study we set a size for the imaging aperture according to the results of the first study and look at the effect of varying the amount of Poisson noise in the images by increasing the exposure or the imaging time. The results from both studies are then compared with theoretical curves for the two observer models.

EXPERIMENTAL METHODS

Model for Imaging System and Signal

Radionuclide imaging is a technique that uses gamma-ray-emitting tracers to image regions of interest within the body. The basic imaging process in nuclear medicine is the projection of a radioactive three-dimensional object onto a two-dimensional (2D) detector plane by use of an aperture between the object and the detector. Since the radiation is gamma rays, there is no diffraction, and the image properties are determined by simple shadow casting.

We assume in this work that we are interested in only a thin slice of the object and therefore that the object is also a planar radioactive emitter. With the assumption of pla-

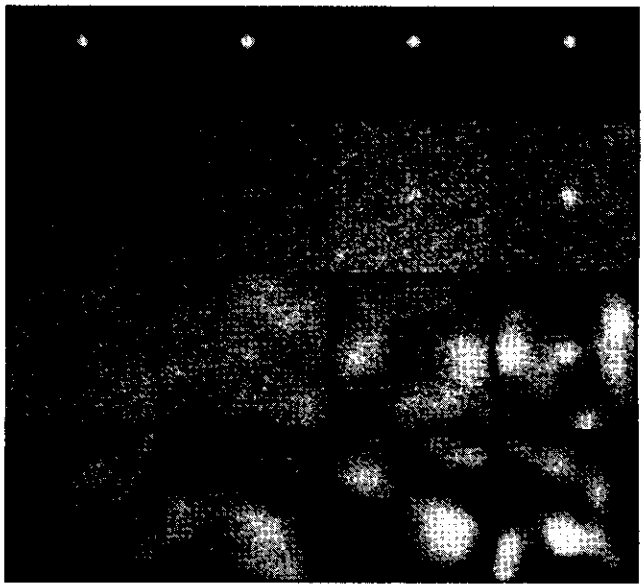

Fig. 2. Illustrative images of a signal on various backgrounds and imaged with various exposure times. The top row shows the signal ($r_s = 5.66$ pixels) that is present in the images below the signal. The exposure time increases from left to right with T equal to 1, 3, 10, and 50 s, while the lumpiness increases from top to bottom with $W_f(0)$ equal to 0, 1.3×10^5, and 8.2×10^5 counts^2/(s pixel). The contrast of the signal on the background was 10% before imaging.

nar imaging, we also assume that the imaging system is linear and shift invariant. For a review of image formation by a simple pinhole aperture and a discussion of the validity of these assumptions, see Barrett and Swindell.[26]

Because the studies presented in this paper are intended to have applications in nuclear medicine, we choose to present the parameters in terms of the emitting plane and the geometry of the imaging system. We assume in this paper that a planar emitting source is being imaged onto a detector through a pinhole aperture equidistant between the emitter and the detector, in which case the magnification of the system is unity. The image $g(\mathbf{r})$ is related to the object $f(\mathbf{r})$ by

$$g(\mathbf{r}) = \kappa T f(\mathbf{r}) * t(\mathbf{r}), \tag{1}$$

where $\mathbf{r}$ is a 2D vector, κ (1/mm^2) is a geometric parameter that is related to the distance from the source to the detector, T (seconds) is the exposure time, $t(\mathbf{r})$ is the aperture transmittance (as projected onto the image plane), and the asterisk denotes 2D convolution.

The object $f(\mathbf{r})$ consists of a signal component and a background. The signal in this work has a 2D Gaussian shape with a half-width measured at the 1/e point of r_s (millimeters) and a strength of a_s (total emitted photons per second). The pinhole aperture is also taken to have a Gaussian transmission profile, with 1/e half-width r_p.

The subscript g is used to specify the parameters related to the image plane. The signal strength and width in the image plane are given as a_{sg} (detected photons or counts) and r_{sg}, respectively. These parameters are related to the object-plane parameters by

$$a_{sg} = \pi\kappa T a_s r_p^2, \qquad r_{sg} = (r_s^2 + r_p^2)^{1/2}. \tag{2}$$

Mathematical Description of a Lumpy Background

In many detectability studies, a signal such as the one just described is superimposed upon a spatially uniform background. In this work, however, the spatial inhomogeneity of the background is the primary concern. The increase in complexity that is due to the variability in the background can be achieved in many different ways, but only certain models will lead to a description that is mathematically tractable.

We make several assumptions to simplify the mathematics. First, we assume that the background is a wide-sense stationary process, where the autocorrelation function is a function of only the distance r between two observation points. Second, we assume that the background autocorrelation function is a Gaussian function of the form

$$R_f(\mathbf{r}) = \frac{W_f(0)}{2\pi r_b^2} \exp(-|\mathbf{r}|^2/2r_b^2), \tag{3}$$

where r_b is the correlation length of the autocorrelation function and $W_f(0)$ is the value of the power spectrum at zero frequency. The subscript f here emphasizes the fact that the autocorrelation function refers to the object $f(\mathbf{r})$ rather than to the image $g(\mathbf{r})$. After imaging, we will refer instead to R_g and W_g. For stationary statistics, the power spectrum $W_f(\boldsymbol{\rho})$ is the Fourier transform of the autocorrelation function, so that

$$W_f(\boldsymbol{\rho}) = W_f(0)\exp(-2\pi^2 r_b^2|\boldsymbol{\rho}|^2), \tag{4}$$

where $\boldsymbol{\rho}$ is the 2D frequency variable in the Fourier domain conjugate to $\mathbf{r}$. The scheme used to simulate the images for the psychophysical studies, in which the images will have the appropriate stationary statistics and Gaussian autocorrelation function, will now be described.

Lumpy-Background Simulations

Two simple approaches to the simulation of lumpy backgrounds have been described in detail by Rolland.[24] One of them (the one used in this paper) is to simulate uncertainty in the background by randomly superimposing Gaussian functions upon a constant background of strength B_0 over the object space. We will often refer to these Gaussian functions as Gaussian blobs or simply blobs. To keep the mathematics simple, we assume here that the Gaussian blobs are of constant amplitude $b_0/\pi r_b^2$ and constant half-width r_b. A background object formed with these Gaussian blobs can be described mathematically as the sum of two terms: a constant term and a term that is the convolution of a set of delta functions, of equal amplitude and randomly located in the object space, with a Gaussian function of constant strength and width. The lumpy component of the background, denoted $b(\mathbf{r})$, is then given by

$$\begin{aligned} b(\mathbf{r}) &= \left[\sum_{j=1}^{K} \delta(\mathbf{r} - \mathbf{r}_j)\right] * \left[\frac{b_0}{\pi r_b^2} \exp\left(-\frac{|\mathbf{r}|^2}{r_b^2}\right)\right] \\ &= \sum_{j=1}^{K} \frac{b_0}{\pi r_b^2} \exp\left(-\frac{|\mathbf{r} - \mathbf{r}_j|^2}{r_b^2}\right), \end{aligned} \tag{5}$$

where r_j is a random variable uniformly distributed over the object area and K is the number of blobs in the background. Note that r_b is the 1/e width of the blobs as well as the correlation length (defined as a standard deviation) of R_f.

The description of a nonuniform background given by Eq. (5) is not sufficient to yield a Gaussian autocorrelation function. The calculation of the autocorrelation function, presented in detail in Appendix A, shows that the number of blobs K must itself be a random variable with the mean of K equal to its variance. This can be seen clearly by simple inspection of Eq. (A12), where the expression for R_f reduces to a Gaussian function if the last two terms cancel. We thus chose K to be Poisson distributed for this condition to be satisfied. The expression for R_f (or W_f) given by Eq. (A13) [or Eqs. (A14) and (A15)] is a complete description of the second-order statistics of the lumpy backgrounds thus generated. The derivations given in Appendix A lead to a measure of lumpiness given by Eq. (A15) as

$$W_f(0) = \frac{\overline{K}}{A_d} b_0^2, \tag{6}$$

where A_d is the detector area, $\overline{K}/A_d$ is the mean number of blobs per detector area (in pixels), and b_0 is the strength of the blobs in units of counts. The lumpiness is then expressed in units of counts^2/(s^2 pixel). Note that lumpiness as defined is a function of only the mean number of blobs per unit area and the strength of the blobs, not of their actual size or shape. The size or the shape of the background blobs is an important factor, however, but only in relation to the size and the shape of the signal to be detected.

The first-order statistics can be expressed as the expected value of the background over the ensemble of objects. The mean level $\overline{B}$ in the object is the sum of two terms, and its expression is given by

$$\overline{B} = B_0 + \frac{b_0}{A_d}\overline{K}. \tag{7}$$

Note that B_0 is in units of counts/(s pixel), $\overline{K}/A_d$ is in units of counts/pixel, and b_0 is in units of counts/s. The mean background $\overline{B}$ is then expressed as the number of counts/(s pixel).

The background parameters, like the signal parameters, are easily referred to the image plane. By analogy to Eq. (1),

$$a_{bg} = \pi\kappa T b_0 r_p^2, \qquad r_{bg} = (r_b^2 + r_p^2)^{1/2}, \tag{8}$$

$$B_{0g} = \pi\kappa T B_0 r_p^2. \tag{9}$$

In the studies reported here, these image parameters were used to compute the mean number of counts at each pixel in a set of digital images in which each pixel represented a physical width of 0.425 mm. Since the Gaussian functions used for the signal and the background have Fourier transforms that fall off rapidly, the sampling error was negligible, and the continuous expressions used in this paper were an accurate representation of the digital images. The images were created without noise, but then the appropriate amount of Poisson noise, as determined by κT, was added.

Parameter Choice for Psychophysical Studies

In the first study, aimed at studying the effects of spatial resolution, the assigned parameter values for the emitted signal were $a_s = 6 \times 10^4$ counts/s and $r_s = 5.66$ pixels or 2.4 mm. The fixed level B_0 was set to 3×10^3 counts/(s pixel), and the mean number of blobs $\overline{K}$, which was actually the mean of a Poisson random process, was assigned the values 0, 50, and 100 when $W_f(0)$ took the values 0, 1.2×10^8, and 2.4×10^8 counts^2/(s^2 pixel), respectively. The strength of the blobs b_0, on the other hand, was kept constant and equal to 2×10^5 counts/s. The half-width of the background blob r_b was three times the half-width of the signal ($r_b = 3r_s$). The value of the mean background changed with the amount of lumpiness as given by Eq. (9). The signal contrast, defined as $s(0)/\overline{B}$, where $s(r)$ is the signal, was 19.9%, 16.1%, and 14.1% as $W_f(0)$ increased. The imaging aperture was chosen to yield a Gaussian point-spread function of half-width r_p. This choice is only a pure mathematical convenience with respect to the computation of the theoretical predictions. The exposure time of the imaging system was set to be 1 s, while the efficiency factor κ that takes into account the geometry of the system was set to 10^{-3}.

In the second study, in which we studied the exposure-time dependence, we assigned a value of 2.5×10^3 counts/s to a_s and 5.66 pixels or 2.4 mm to r_s. We set the mean number of blobs to be a constant of value 50 and the strength of the blob b_0 to be the variable parameter with b_0 equal to 0, 6.5×10^3, and 1.6×10^4 counts/s when $W_f(0)$ equaled 0, 1.3×10^5, and 8.2×10^5 counts^2/(s^2 pixel), respectively. The contribution of the fixed dc level to the mean background level was 250, 230, and 200 counts/(s pixel) as the lumpiness increased from 0 to 8.2×10^5 counts/(s^2 pixel). The mean background level was then constant of value 250 counts/(s pixel), and the contrast of the signal on the background was 10% for the three values of lumpiness.

Protocol

For each study we determined human performance for the case of a uniform background and two nonzero values of lumpiness. We used four values for the ratio of the aperture size to the signal size r_p/r_s in the first study and three or four values for the exposure time in the second study, as we describe in more detail below. We thus designed 12 and 11 experiments in the first and the second studies, respectively.

In each experiment 70 images were generated; 35 images had a signal located in the center of the image and superimposed upon either a uniform or a lumpy background, while the other 35 had similar backgrounds but no signal. Among the 70 images of each experimental set (among the 12 or 11 sets), 6 images were extracted to constitute a training set for the observers. For the first study, the training set was thus composed of 72 images (12 times 6), while 66 images (11 times 6) were used to train the observers for the second study. The remaining 64 images in each set were then used as the test sample to evaluate human-observer performance.

Once Poisson noise was added to the computer-simulated images, eight bits of gray level were used to display the images. The images were displayed as a 128 × 128-pixel array using the gray-level-to-brightness transfer curve shown in Fig. 3. One image was displayed at a time and covered 5.4 cm × 5.4 cm on the display, so that each pixel measured 0.42 mm × 0.42 mm. The contrast and the brightness levels of the display monitor were fixed during the study, and the observers were not allowed to vary them to optimize their performance. The brightness of the displayed images was ~18 fL. The observers viewed the images binocularly at a distance of ~50 cm and were required to wear their usual corrective lenses.

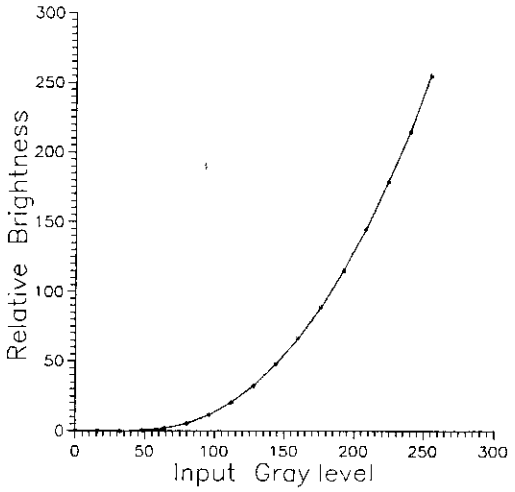

Fig. 3. Plot of the measured relative brightness versus the displayed gray levels at the cathode-ray tube screen. The measurements were done with a photodiode–55-mm-camera assembly looking at a 16 × 16 pixel array of gray-level values ranging from 0 to 255. The 16 × 16 pixel array was centered in a 128 × 128-pixel array of gray-level value 128. The display monitor was driven by a PCvision board.

Ten different observers participated in each study, each performing 12 and 11 experiments for studies I and II, respectively. The observers did not have any information on the number of occurrences of the signal. In each study, the images from the experiments were displayed in a random order. The observer was presented a single stimulus on each trial, that is, a noisy image with or without the signal. The observers were instructed to rate their certainty on a six-point scale, and the responses were recorded and analyzed by using receiver operating characteristic analysis.[27-30] The performance measure used was the index of detectability d_a, defined by

$$d_a^2 = \frac{[\langle\lambda(g)|1\rangle - \langle\lambda(g)|0\rangle]^2}{P_0 \operatorname{var}(\lambda(g)|0) + P_1 \operatorname{var}[\lambda(g)|1]}, \tag{10}$$

where $\langle\lambda(g)|k\rangle$ is the mean of the test statistic $\lambda(g)$ given that the data g come from class $k = 0$ (signal absent) or class $k = 1$ (signal present), while $\operatorname{var}[\lambda(g)|k]$ is the corresponding conditional variance. The probability of the occurrence of the signal, P_2, was set to 1/2; therefore $P_1 = P_2 = 1/2$. If $\lambda(g)$ obeys Gaussian statistics, d_a is related to the area under the receiver operating characteristic curve (AUC) by

$$\mathrm{AUC} = \frac{1}{2} + \frac{1}{2}\operatorname{erf}\left(\frac{d_a}{2}\right), \tag{11}$$

where erf( ) is the error function. The index d_a was then calculated from the AUC values for each observer by using Eq. (11), and a mean value of d_a was obtained by averaging over the different observers.

Theoretical Predictions

As mentioned above, a detailed analytical solution to the lumpy background problem has been reported by Myers *et al.*[25] We review this analysis here and point out the key assumptions that made this problem tractable. Basically, one way of looking at the imaging procedure is to consider the imaging of one realization of the object, that is, a lumpy background with or without the signal present, through a pinhole aperture in a purely geometric or deterministic fashion. The deterministic image then formed should be taken as the mean of a Poisson random process.

In computing the Hotelling-observer performance known as the Hotelling trace criterion J, all we need to determine are the first- and the second-order statistics on the data as defined by the two scatter matrices S_1 and S_2, since J is defined as

$$J = \operatorname{Tr}(S_2^{-1}S_1). \tag{12}$$

The interclass scatter matrix S_1 is a measure of the separation of the mean values of the two classes (signal being present or absent, respectively), while the intraclass scatter matrix S_2 is the mean covariance matrix averaged over the two classes.[23,25] To evaluate S_2, the key assumption is that the background is a stationary random process, which means that the covariance matrices that go into S_2 are diagonalized by a discrete Fourier transform. Moreover, the detectability index d_a associated with the Hotelling observer and referred to as d_{Hot} is related to J by

$$J = P_1P_2d_{\mathrm{Hot}}^2, \tag{13}$$

where d_{Hot} may then be expressed in our study as an integral over the Fourier domain[25] of the form

$$(d_{\mathrm{Hot}})^2 = \int_\infty d^2\rho \frac{|\tilde{s}(\rho)|^2|\tilde{H}(\rho)|^2}{[\bar{B}_g + |\tilde{H}(\rho)|^2W_f(\rho)]}, \tag{14}$$

where $\tilde{s}(\rho)$ is the Fourier transform of the signal and $\tilde{H}(\rho)$ is the transfer function of the system.

In computing the NPW observer, we need to perform a matched filter of the data with the expected difference signal under the two hypotheses. The filter itself does not take into account either the Poisson process or the background noise, but both noise processes will be manifest in the expression of the variance of the filter output. Here again, because of the stationarity of the statistical processes involved, the detectability index d_a associated with the NPW observer and referred to as d_{NPW} may be expressed with integrals in the Fourier domain as

$$(d_{\mathrm{NPW}})^2 = \frac{\left[\int_\infty d^2\rho|\tilde{s}(\rho)|^2|\tilde{H}(\rho)|^2\right]^2}{\bar{B}_g\int_\infty d^2\rho|\tilde{s}(\rho)|^2|\tilde{H}(\rho)|^2 + \int_\infty d^2\rho|\tilde{s}(\rho)|^2|\tilde{H}(\rho)|^4W_f(\rho)}. \tag{15}$$

Variation with Aperture Size

Given the set of parameters described above, we computed the performance of the Hotelling and the NPW observers as a function of the relative pinhole size r_p/r_s, which varied from 0.2 to 4. The predictions of those two observers are given in Fig. 4. The top curve represents the performance of both observers for the case of a uniform background where quantum noise is the limiting factor.

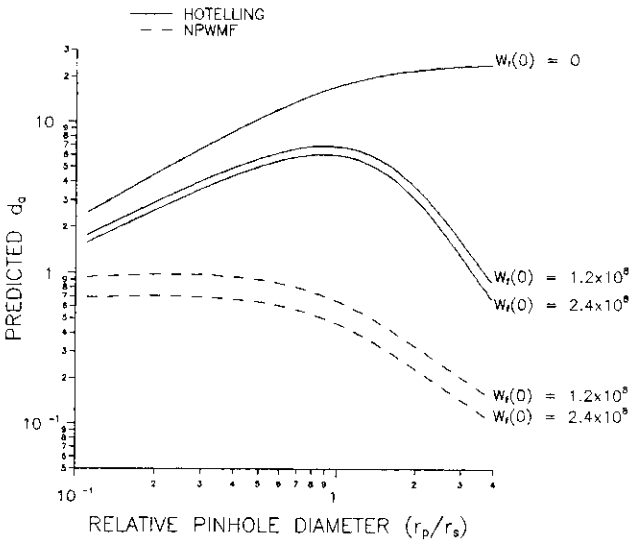

Fig. 4. Plot of the detectabilities predicted by the Hotelling and the NPW observers for the detection of a low-contrast signal on uniform [$W_f(0) = 0$] and nonuniform [$W_f(0) \neq 0$] backgrounds as a function of the size of the pinhole aperture r_p. The width of the signal is 5.66 pixels, and the contrasts of the signal are 19.9%, 16.5%, and 14.1% as the lumpiness increases, since the dc background level is kept constant (3000 counts/(s pixel) as we increase the lumpiness, but the mean background level is a function of both the dc background level and the lumpiness [see Eq. (6)]. The mean numbers of blobs are 0, 50, and 100 as $W_f(0)$ increases, while the strength of the blob b_0 is kept constant (2×10^5 counts/s). NPWMF, NPW matched filter.

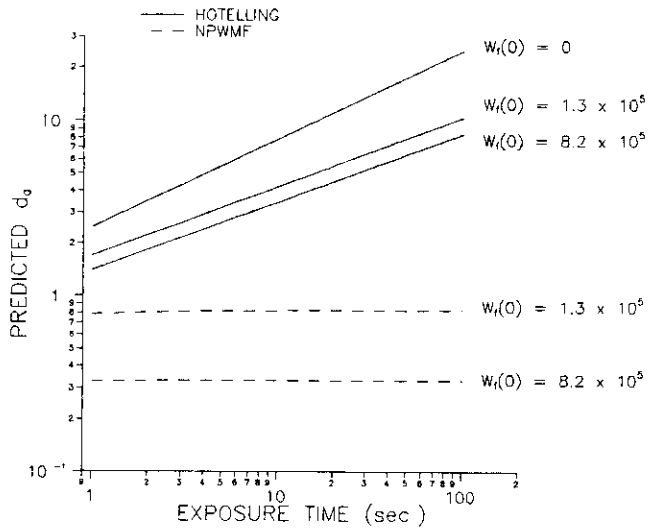

Fig. 5. Plot of the detectabilities predicted by the Hotelling and the NPW observers for the detection of a low-contrast signal on uniform [$W_f(0) = 0$] and nonuniform [$W_f(0) \neq 0$] backgrounds as a function of the exposure time T. The width of the signal is 5.66 pixels, and the contrast of the signal is 10% before imaging. As the amount of lumpiness increases, the dc background levels are 250, 230, and 200 counts/(s pixel) such that the mean background level is a constant $B = 250$ counts/(s pixel). The mean number of blobs is 50, and the strengths of the blobs are 0, 6.55×10^3 and 1.64×10^4 counts/s as $W_f(0)$ increases. NPWMF, NPW matched filter.

The performance of both observers, in the case of a uniform background, is equivalent to the performance of the ideal observer, and therefore the two resulting theoretical curves perfectly overlap as shown. The two middle curves correspond to the Hotelling performance as the amount of lumpiness increases, while the two lower curves predict the NPW-observer performance for the same amounts of lumpiness as used for the Hotelling observer. Given this set of theoretical curves that indicate different predictions for the Hotelling and the NPW observers, we should be able to find which model best predicts human performance.

The psychophysical study was based on the same set of parameters as described for the theoretical predictions but with r_p/r_s limited to four values, 0.2, 0.8, 1.5, and 3.4.

Variation with Exposure Time

Given the set of parameters described above for this study, we set the aperture size r_p to 5.66 pixels, so that $r_p = r_s$. We then let the counting time or the exposure time vary from 1 to 100 s, and we computed the performances of our two theoretical observers, the Hotelling and the NPW observers. Increasing T increases the overall counts, and thus it is equivalent to a decrease of the relative Poisson noise at the pixel. The performances are depicted in Fig. 5, where we plot the detectability index d_a as a function of exposure time. The predictions show an increase of the Hotelling performance as a function of time for both the uniform and the nonuniform backgrounds. The predicted values of the slopes are approximately 0.5 and 0.4 for the uniform and the nonuniform backgrounds, respectively. The performance of the NPW observer, on the other hand, is constant with increasing counting time. The detectability of the signal by this observer is thus limited by the background variation rather than by the Poisson statistics, and we say that the performance is conspicuity limited for the chosen values of lumpiness and exposure times. (In the radar literature, this condition is referred to as clutter limited.) The saturation of performance with increasing exposure time can be better seen if we refer back to the theoretical curves presented by Myers *et al.*[25] Figure 8 of that paper shows clearly the transition between quantum-limited and conspicuity-limited performance. Figure 5 of the present paper, on the other hand, does not show this transition, simply because it occurs for T smaller than the values plotted.

The parameters chosen to simulate the images were identical to those used in the theoretical predictions but with exposure times limited to the values of 1, 3, 10, and 20 s for $W_f(0) = 0$; the values were 1, 3, 10, and 50 s for $W_f(0) = 1.3 \times 10^5$ and 1, 3, 10, and 100 s for $W_f(0) = 8.2 \times 10^5$ counts^2/(s^2 pixel).

RESULTS

Variation with Aperture Size

The results of the first psychophysical study are given in Fig. 6, which plots the average detectability index d_a versus r_p/r_s. Each point corresponds to an average of the performance of each observer over the 10 observers. The estimated standard deviation at each point is given by the mean rms error between the observers.

We first note that for uniform backgrounds the performance of the human observer does not increase indefinitely as predicted by the ideal observer; rather, it presents an optimum when r_p is approximately matched to the size of the signal r_s. As the lumpiness increases, the performance of the human observer decreases and the optimum aperture size decreases, a fact that is better seen as the lumpiness increases from 0 to 1.2×10^8. From just a glance at the experimental data, we see a good agree-

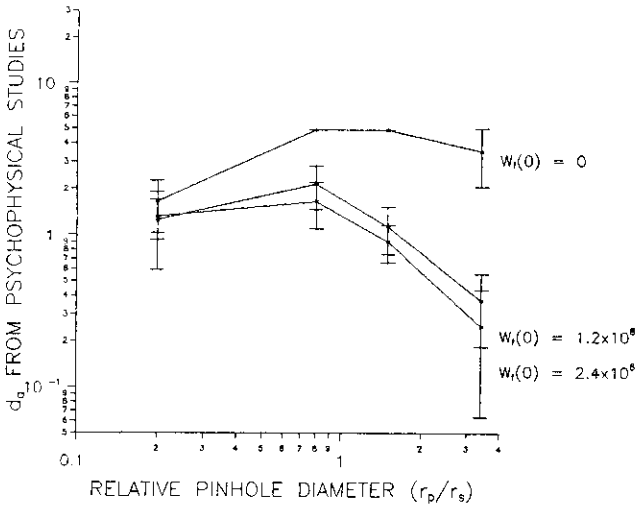

Fig. 6. Values of detectabilities obtained from the psychophysical studies for the detection of a low-contrast signal on uniform [$W_f(0) = 0$] and nonuniform [$W_f(0) \neq 0$] backgrounds as a function of the size of the pinhole aperture. The values of the parameters used to generate the computer-simulated images are the same as those given in the caption to Fig. 4. Four values of the size of the pinhole aperture r_p relative to the size of the signal r_s are chosen in this case: r_p/r_s equal to 0.2, 0.8, 1.5, and 3.4. The lines shown are simply the lines connecting the data points.

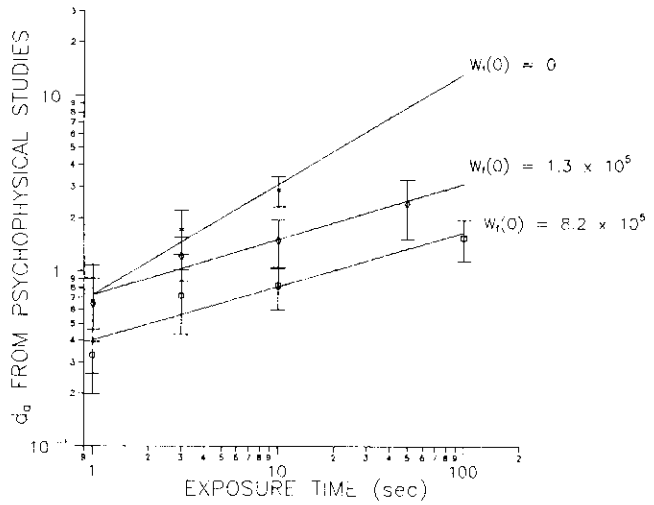

Fig. 7. Values of detectabilities obtained from the psychophysical studies for the detection of a low-contrast signal on uniform [$W_f(0) = 0$] and nonuniform [$W_f(0) \neq 0$] backgrounds as a function of the exposure time T. The values of the parameters used to generate the computer-simulated images are the same as those given in the caption to Fig. 5. Four values of T are chosen: T equal to 1, 3, 10, 50, and 100 s as shown on the graph.

ment between the experimental data and the predictions in the performance of the Hotelling observer. We do not in any case expect a perfect match of the experimental data with theory since the efficiency of the human observer, which is not only a function of the amount of training of the human observer but also a function of some inherent properties of the visual system, must be taken into account. In fact, if we overlap the experimental results on the theoretical curves with an upward shift of the experimental curves to take into account the efficiency of the human observer, we find a good agreement of the data with the Hotelling-observer predictions, while the NPW observer fails to predict human performance for the detection of a signal in a nonuniform background. The efficiency of the human observer compared with that of the Hotelling observer is approximately 10% in this experiment. For a review of the concept of human efficiency see, for example, the paper by Tanner and Birdsall.[31]

Another interesting point from Fig. 6 is that the absolute degradation of performance resulting from the background inhomogeneity is closely predicted by the Hotelling model and not at all by the NPW model. The Hotelling and the human observers are much less influenced by the inhomogeneity than is the NPW observer.

Variation with Exposure Time

The results of the exposure-time study are presented in Fig. 7. The results show an increase in performance as a function of the exposure time regardless of the amount of lumpiness. These results show that the NPW observer does not predict human performance for the detection of a known signal in a nonuniform background. Moreover, if we overlap the experimental results with the theoretical predictions of the Hotelling observer, we see that the Hotelling observer is again a good predictor of human performance within the efficiency factor of the human observer. Both the human and the Hotelling observers can benefit from increased exposure time, while the NPW observer cannot (for the range of times considered here).

Since we have 30 or 40 data points per regression line (10 observers with three or four values of T), we performed a t test with 29 or 39 degrees of freedom to test the hypothesis that the slopes of the experimental (log–log) regression lines shown in Fig. 7 are equal to the slopes of the theoretical lines predicted by the Hotelling observer. We note that, for a given lumpiness value, the variances at each point on the regression line are different as the time varies. To test our hypothesis of equality of the slopes of the regression lines using the t test, we needed first to transform the data in such a way that the variances became equal. Following Deaton,[32] we divided the values of the data points by the variances, so that the data were transformed into unit variances. We found that the hypothesis of equality can be accepted at a significance level of better than 8% ($P = 0.08$) for the two lower regression lines. The slope of the regression line corresponding to no lumpiness was found, on the other hand, to be greater than the predicted value according to the test performed.

DISCUSSION

If we compare human performance with the predictions of the Hotelling observer, there is a significant deviation of the experimental data from the theoretical curves only in the case of a uniform background. As can be seen from Fig. 6, the results unambiguously show in that case that the performance is optimal when r_p takes a value that is between approximately 0.8 and 1.5 times the size of the signal. For larger apertures, the performance starts to decrease slowly instead of saturating as predicted by the Hotelling and the NPW observers, which are in this case equivalent to the ideal observer.

Such an observation was also pointed out by Tsui *et al.*[33] when the task was the discrimination between two tumor activity distributions embedded in a uniform background. For their experimental data to agree with the theoretical predictions of the ideal observer, Tsui *et al.* made the assumption that the efficiency of the human observer itself was a linear function of the aperture size. By referring back to Eqs. (1) and (2), we see that increasing r_p makes the ratio of r_{sg} and r_{bg} closer to 1. Tsui *et al.* then found good agreement of the data with the predicted values by taking this varying efficiency factor into account. We could also take such an approach to match better our experimental data to the theoretical data in the case of uniform backgrounds. However, as the complexity in the background increases, the efficiency of the human observer can be not only a function of the aperture size but also a function of the lumpiness in the background, so the problem becomes quite complex. Note, however, that, even with the assumption that the efficiency of the human observer is constant as a function of aperture size and as a function of lumpiness in the background, our experimental results are in good agreement with the predictions of the Hotelling observer.

A similar drop in efficiency was also reported by White *et al.*[34] in a human performance study designed to select the optimum set of parameters to describe a collimator. The task that they proposed was the detection of tumors of various sizes and locations in computer-simulated liver scans. They found a significant drop in efficiency at large aperture sizes for the human observer.

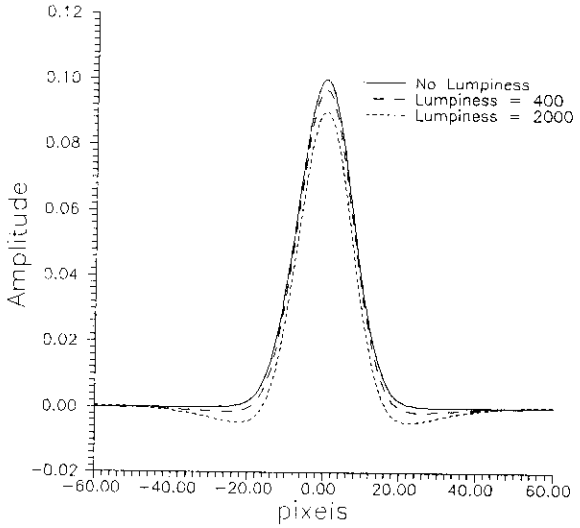

Fig. 8. Example of the profile of the Hotelling feature operator along a radial axis in the space domain for the detection of a Gaussian signal on one uniform and two nonuniform backgrounds. Lumpiness is equivalent to $W_f(0)$. The mean value of the background is 610 counts/(s pixel). The signal width was 10 pixels, and the background autocorrelation length was 30 pixels.

According to our experience,[24,35] we postulate that such a drop resulting from the blurring effect of a large aperture can be corrected for by processing the images with a high-pass filter before display.

Another small deviation of the experimental data from the theoretical data was found when we looked at the effect of the exposure time on the performance of the human observer, again for the case of a uniform background. Further investigations should be carried out for us to understand fully the reason for this small discrepancy. Despite this observation, the results show good agreement of the experimental data with the Hotelling model as the exposure time and the lumpiness increase.

Although further investigations could highlight some small discrepancies between the human and the Hotelling performances, we have shown that the Hotelling observer is a good measure of image quality for the nonuniform background problem.

This agreement in performance between the Hotelling and the human observers can perhaps be explained by comparing the shape of the feature operator of the Hotelling observer with the shape of some receptive fields found in the human visual system. The shape of the feature operator of the Hotelling observer for different values of lumpiness resembles a difference-of-Gaussians (DOG) type of filter. Moreover, this filter is found to be adaptive with respect to the background structure. An example of the feature operator associated with the Hotelling observer is shown in Fig. 8 for three values of lumpiness. We note that these filters resemble in shape the on-center and the off-surround receptive fields found in the human visual system, a resemblance that might explain the correlation in the performance of the Hotelling and the human observers. The feature operator of the NPW observer, on the other hand, possesses only an on-center structure since the function of the NPW observer is to match filter the signal.

The fact that the NPW observer does not predict human performance can be puzzling, however, if we recall the work of Myers *et al.*[36] in which they investigated human performance for the detection of a disk signal superimposed upon a uniform background but embedded in correlated noise. They showed that the NPW observer was the best predictor of human performance and that the ideal observer (equivalent to the Hotelling observer in this case) gave much poorer correlation. In a later paper, Myers and Barrett[37] attempted to explain their data by introducing the concept of the channelized ideal observer, which is an ideal observer except for the fact that it has access to the data only after their processing through some finite spatial-frequency bands referred to as channels.[38] Myers and Barrett showed that the predictions of the NPW and the channelized-ideal models were virtually indistinguishable over a wide range of parameter values.

The findings in the present paper as well as those of Myers *et al.*[36,37] suggest the derivation of what we could call a channelized Hotelling observer. Such a model might be found to predict human performance in both correlated noise but uniform background and uncorrelated noise but spatially varying background. Work in this direction is currently in progress at the University of Arizona.

CONCLUSION

We have measured the effect of inhomogeneity in the background on the detectability of a Gaussian signal imaged through a pinhole aperture of finite resolution and corrupted by Poisson noise. Our results show that the variations in performance of the human observer with respect to varying aperture size and exposure time can be well predicted by the optimum linear discriminant known as the Hotelling observer, although the efficiency of the human observer with respect to the Hotelling observer was only approximately 10%. The NPW observer, which performs a simple matched-filter operation, fails to predict the variation in performance of the human observer with respect to the same two parameters for the case of spatially varying backgrounds.

These findings may perhaps be explained by the fact that the feature operator for the Hotelling observer resembles in shape the center–surround receptive fields typically found in the human visual system. The NPW observer does not incorporate this center–surround behavior, and this observer can therefore mistake background nonuniformities for signal. Since the Hotelling receptive fields have the ability to adapt to the lumpiness and the noise level in the image, the Hotelling observer can optimally estimate the local background, avoiding the confusion between signal and background; evidently humans can do so as well.

APPENDIX A: DERIVATION OF THE EXPRESSION FOR THE AUTOCORRELATION FUNCTION OF LUMPY BACKGROUNDS

For the case of lumpy backgrounds as described in this paper, the random variable used to describe the lumpiness in the background is given by

$$b(\mathbf{r}) = \left[\sum_{i=1}^{K} \delta(r - r_i)\right] * y(\mathbf{r}), \tag{A1}$$

with

$$y(\mathbf{r}) = \frac{b_0}{\pi r_b^2} \exp[-|r|^2/(r_b^2)], \tag{A2}$$

where K is the number of Gaussian blobs in the background and r_i is a uniformly distributed random variable that specifies the location of the ith blob. The expression for the autocorrelation of the background is given as a function of $b(\mathbf{r})$ by

$$R_f(\mathbf{r}' - \mathbf{r}'') = \langle [b(\mathbf{r}') - \langle b(\mathbf{r}')\rangle_f][b(\mathbf{r}'') - \langle b(\mathbf{r}'')\rangle_f]\rangle_f, \tag{A3}$$

where $\mathbf{r}'$ and $\mathbf{r}''$ are 2D position vectors and $\langle b(\mathbf{r}')\rangle_f$ is the expectation value of $b(\mathbf{r}')$ averaged over the ensemble of objects that constitute the lumpy backgrounds. The expression for R_f given by Eq. (A3) can then be expressed as the sum of four terms as

$$\begin{aligned} R_f = {} & \langle b(\mathbf{r}')b(\mathbf{r}'')\rangle_f + \langle\langle b(\mathbf{r}')\rangle_f\langle b(\mathbf{r}'')\rangle_f\rangle_f \\ & - \langle b(\mathbf{r}')\langle b(\mathbf{r}'')\rangle_f\rangle_f - \langle\langle b(\mathbf{r}')\rangle_f b(\mathbf{r}'')\rangle_f, \end{aligned} \tag{A4}$$

which reduces from the linearity of the expectation operation to only two terms as

$$R_f = \langle b(\mathbf{r}')b(\mathbf{r}'')\rangle_f - \langle b(\mathbf{r}')\rangle_f\langle b(\mathbf{r}'')\rangle_f. \tag{A5}$$

In carrying out the calculations for R_f we rewrite R_f as

$$R_f = \langle R_{f|k}\rangle_k \tag{A6}$$

with

$$R_{f|k} = \langle b(\mathbf{r}')b(\mathbf{r}'')\rangle_{f|k} - \langle b(\mathbf{r}')\rangle_{f|k}\langle b(\mathbf{r}'')\rangle_{f|k}, \tag{A7}$$

where the notation indicates that we first average over the random positions r_j for a fixed number of blobs K and then average over K itself.

The second term of Eq. (A7) is given by

$$\begin{aligned} \text{term2} &= \langle b(\mathbf{r}')\rangle_{f|k}\langle b(\mathbf{r}'')\rangle_{f|k} \\ &= \left\langle \sum_{i=1}^{K} y(\mathbf{r}' - \mathbf{r}_i)\right\rangle_{f|k} \left\langle \sum_{i=1}^{K} y(\mathbf{r}'' - \mathbf{r}_i)\right\rangle_{f|k} = K^2\frac{b_0^2}{A_d^2}. \end{aligned} \tag{A8}$$

Let us now look at the first term of Eq. (A7). It can be explicitly written as

$$\begin{aligned} &\langle b(\mathbf{r}')b(\mathbf{r}'')\rangle_{f|k} \\ &= \left\langle \sum_{i=1}^{K}[\delta(\mathbf{r}' - \mathbf{r}_i) * y(\mathbf{r}')] \sum_{j=1}^{K}[\delta(\mathbf{r}'' - \mathbf{r}_j) * y(\mathbf{r}'')]\right\rangle_{f|k} \\ &= \left\langle \sum_{i=1}^{K} y(\mathbf{r}' - \mathbf{r}_i) \sum_{j=1}^{K} y(\mathbf{r}'' - \mathbf{r}_j)\right\rangle_{f|k} \\ &= \int d^2r_1 pr(\mathbf{r}_1)\ldots \int d^2r_K pr(\mathbf{r}_K) \sum_{i=1}^{K} y(\mathbf{r}' - \mathbf{r}_i) \sum_{j=1}^{K} y(\mathbf{r}'' - \mathbf{r}_j), \end{aligned} \tag{A9}$$

where $pr(\mathbf{r}_i)$ is the probability density associated with the random variable $\mathbf{r}_i$. If $i = j$, it can be shown that each term of the sums over i and j contributes in the same fashion to term 1. The details of this calculation can be found in the paper by Rolland,[24] who adapted the theory of Barrett and Swindell[26] to the case of lumpy backgrounds. Since there are K terms such that $i = j$, the first term of Eq. (A7) becomes, for $i = j$,

$$\text{term1}(i = j) = \frac{K}{A_d}\frac{b_0^2}{2\pi r_b^2} \exp[-|\mathbf{r}|^2/(2r_b^2)]. \tag{A10}$$

In a similar way, since there are $(K^2 - K)$ terms with $i \neq j$, the contribution of the terms $i \neq j$ to the first term of Eq. (A7) is given by

$$\text{term1}(i \neq j) = (K^2 - K)\frac{b_0^2}{A_d^2}. \tag{A11}$$

Finally, the expression for the autocorrelation function, that is, the sum of term1 $(i = j)$, term1$(i \neq j)$, and term2 given by Eqs. (A10), (A11), and (A8), respectively, becomes

$$\begin{aligned} R_{f|k} = {} & \frac{K}{A_d}\frac{b_0^2}{2\pi r_b^2} \exp[-|\mathbf{r}|^2/(2r_b^2)] \\ & + (K^2 - K)\frac{b_0^2}{A_d^2} + K^2\frac{b_0^2}{A_d^2}. \end{aligned} \tag{A12}$$

This expression shows that the autocorrelation function is found to be Gaussian only if K satisfies $\langle K^2 - K\rangle = \langle K\rangle$. The second term of Eq. (A12) then cancels with the third term of the equation. If K is a Poisson random variable, $\langle K^2\rangle - \langle K\rangle^2 = \langle K\rangle$, then $\langle K^2 - K\rangle = \langle K\rangle^2$, and the autocorrelation function reduces to

$$R_f(r) = \frac{\overline{K}}{A_d}\frac{b_0^2}{2\pi r_b^2} \exp[-|\mathbf{r}|^2/((2r_b^2)]. \tag{A13}$$

The power spectrum, which is defined as the Fourier transform of the autocorrelation function for the stationary random process, is given by

$$\begin{aligned} W_f(\rho) &= \frac{\overline{K}}{A_d} b_0^2 \exp(-2\pi^2 r_b^2|\boldsymbol{\rho}|^2) \\ &= W_f(0)\exp(-2\pi^2 r_b^2|\boldsymbol{\rho}|^2), \end{aligned} \tag{A14}$$

with

$$W_f(0) = \frac{\overline{K}}{A_d} b_0^2. \tag{A15}$$

We use $W_f(0)$ as the measure of the lumpiness in the background. Note that $W_f(0)$ is a measure of counts^2/(s^2 pixel).

ACKNOWLEDGMENTS

The authors acknowledge the late George Seeley for his guidance in designing the psychophysical studies and thank John Denny and Ted Gooley for their help with the statistical analysis of the data. The authors are also grateful to Kyle Myers, Robert Wagner, Arthur Burgess, and Jie Yao for their helpful and stimulating discussions throughout this research. We also thank all the people who participated in the observer studies for their patience, enthusiasm, and strong cooperation. This research was supported by the National Cancer Institute under grants P01 CA23417 and R01 CA52643.

*Present address, Department of Computer Science, University of North Carolina, Chapel Hill, North Carolina 27599.

REFERENCES

1. K. M. Hanson, "Detectability in computed tomographic images," Med. Phys. **6,** 441–451 (1979).
2. H. H. Barrett, J. N. Aarsvold, H. B. Barber, E. B. Cargill, R. D. Fiete, T. S. Hickernell, T. D. Milster, K. J. Myers, D. D. Patton, R. K. Rowe, R. H. Seacat, W. E. Smith, and J. M. Woolfenden, "Applications of statistical decision theory in nuclear medicine," *Information Processing in Medical Imaging* (Plenum, New York, 1988).
3. H. L. Van Trees, *Detection, Estimation, and Modulation Theory* (Wiley, New York, 1968), Vols. I–III.
4. D. B. Green and J. A. Swets, *Signal Detection Theory and Psychophysics* (Wiley, New York, 1966).
5. A. E. Burgess, R. F. Wagner, R. J. Jennings, and H. B. Barlow, "Efficiency of human visual discrimination," Science **214,** 93–94 (1981).
6. A. E. Burgess, R. F. Wagner, and R. J. Jennings, "Human signal detection performance for noisy medical images," in *Proceedings of the IEEE ComSoc International Workshop on Medical Imaging,* IEEE catalog no. 82CH1751-7 (Institute of Electrical and Electronics Engineers, New York, 1982).
7. K. M. Hanson, "Variations in task and the ideal observer," in *Application of Optical Instrumentation in Medicine XI,* G. D. Fullerton, ed., Proc. Soc. Photo-Opt. Instrum. Eng. **419,** 60–67 (1983).
8. A. E. Burgess and H. Ghandeharian, "Visual signal detection. II. Signal-location identification," J. Opt. Soc. Am. A **1,** 906–910 (1984).
9. P. F. Judy and R. G. Swensson, "Detection of small focal lesions in CT images: effects of reconstruction filters and visual display windows," B. J. Radiol. **58,** 137–145 (1985).
10. R. F. Wagner and D. G. Brown, "Unified SNR analysis of medical imaging systems," Phys. Med. Biol. **30,** 489–518 (1985).
11. G. Revesz, H. L. Kundel, and M. A. Graber, "The influence of structured noise on detection of radiologic abnormalities," Invest. Radiol. **9,** 479–486 (1974).
12. R. G. Swensson and P. F. Judy, "Background area effects on feature detectability in CT and uncorrelated noise," presented at the 73rd Annual Meeting of the Radiological Society of North America, Chicago, Ill., 1987.
13. F. L. Engel, "Visual conspicuity and selective background interference in eccentric vision," Vision Res. **14,** 459–471 (1973).
14. B. L. Cole and S. E. Jenkins, "The effect of the variability of background elements on the conspicuity of objects," Vision Res. **24,** 261–270 (1984).
15. U. E. Ruttimann and R. L. Webber, "A simple model combining quantum noise and anatomical variation in radiographs," Med. Phys. **11,** 50–60 (1984).
16. B. M. W. Tsui, C. E. Metz, F. B. Atkins, S. J. Starr, and R. N. Beck, "A comparison of optimum spatial resolution in nuclear imaging based on statistical theory and on observer performance," Phys. Med. Biol. **23,** 654–676 (1978).
17. K. Fukunaga, *Introduction to Statistical Pattern Recognition* (Academic, New York, 1972).
18. Panel on Discriminant Analysis, Classification, and Clustering, "Discriminant analysis and clustering," Stat. Sci. **4,** 34–69 (1989).
19. Z. H. Gu and S. Lee, "Optical implementation of the Hotelling trace criterion for image classification," Opt. Eng. **23,** 727–731 (1984).
20. W. E. Smith and H. H. Barrett, "Hotelling trace criterion as a figure of merit for the optimization of imaging systems," J. Opt. Soc. Am. A **3,** 717–725 (1986).
21. R. D. Fiete, H. H. Barrett, W. E. Smith, and K. J. Myers, "The Hotelling trace criterion and its correlation with human observer performance," J. Opt. Soc. Am. A **4,** 945–953 (1987).
22. H. H. Barrett, "Objective assessment of image quality: effects of quantum noise and object variability," J. Opt. Soc. Am. A **7,** 1266–1278 (1990).
23. R. F. Wagner, D. G. Brown, and C. E. Metz, "On the multiplex advantage of coded source/aperture photon imaging," in *Digital Radiography,* W. R. Brody, ed., Proc. Soc. Photo-Opt. Instrum. Eng. **314,** 72–76 (1981).
24. J. P. Rolland, "Factors influencing lesion detection in medical imaging," Ph.D. dissertation (University of Arizona, Tucson, Arizona, 1990).
25. K. J. Myers, J. P. Rolland, H. H. Barrett, and R. F. Wagner, "Aperture optimization for emission imaging: effect of a spatially varying background," J. Opt. Soc. Am. A **7,** 1279–1293 (1990).
26. H. H. Barrett and W. Swindell, *Radiological Imaging: The Theory of Image Formation, Detection, and Processing* (Academic, New York, 1981), Vols. I and II.
27. J. P. Egan, *Signal Detection Theory and ROC Analysis* (Academic, New York, 1975).
28. C. E. Metz, "ROC methodology in radiologic imaging," Invest. Radiol. **21,** 720–733 (1986).
29. C. E. Metz, "Some practical issues of experimental design and data analysis in radiological studies," Invest. Radiol. **24,** 234–245 (1989).
30. J. A. Swets, "Measuring the accuracy of diagnosis systems," Science **240,** 1285–1293 (1988).
31. W. P. Tanner and T. G. Birdsall, "Definition of d' and η as psychophysical measures," J. Acoust. Soc. Am. **30,** 922–928 (1958).
32. M. L. Deaton, "Estimation and hypothesis testing in regression in the presence of nonhomogeneous error variances," Commun. Statist. Simula. Computation **12,** 45–66 (1983).
33. B. M. W. Tsui, C. E. Metz, and R. N. Beck, "Optimum detector spatial resolution for discriminating between tumor uptake distributions in scintigraphy," Phys. Med. Biol. **28,** 775–788 (1982).
34. T. A. White, H. H. Barrett, E. B. Cargill, R. D. Fiete, and M. Ker, "The use of the Hotelling trace to optimize collimator performance," J. Nucl. Med. **30,** 892 (A) (1989).
35. J. P. Rolland, H. H. Barrett, and G. W. Seeley, "Quantitative study of deconvolution and display mappings for long-tailed point-spread functions," in *Medical Imaging III: Image Processing,* S. J. Dwyer, R. G. Jost, and R. H. Schneider, ed., Proc. Soc. Photo-Opt. Instrum. Eng. **1092,** 17–21 (1989).
36. K. J. Myers, H. H. Barrett, M. C. Borgstrom, D. D. Patton, and G. W. Seeley, "Effect of noise correlation on detectability of disk signals in medical imaging," J. Opt. Soc. Am. A **2,** 1752–1759 (1985).
37. K. J. Myers and H. H. Barrett, "Addition of a channel mechanism to the ideal-observer model," J. Opt. Soc. Am. A **4,** 2447–2457 (1987).
38. M. Sachs, J. Nachmias, and J. Robson, "Spatial-frequency channels in human vision," J. Opt. Soc. Am. **61,** 1176–1186 (1971).